

Donor-Donor'-Acceptor Triads based on [3.3]Paracyclophane with 1,4-Dithiafulvene Donor and Cyanomethylene Acceptor: Synthesis, Structure, Electro- and Photo-physical Properties

Katsuya Sako,^{[a]*} Tomoya Hasegawa,^[a] Hiroyuki Onda,^[a] Michito Shiotsuka^[a], Motonori Watanabe,^[b] Teruo Shinmyozu,^[c] Sachiko Tojo,^[d] Mamoru Fujitsuka,^[d] Tetsuro Majima,^[d] Yasukazu Hirao,^[e] Takashi Kubo,^[e] Tetsuo Iwanaga,^[f] Shinji Toyota,^[g] and Hiroyuki Takemura^[h]

Abstract: Donor-donor'-acceptor triads (**1**, **2**) based on [3.3]paracyclophane ([3.3]PCP) as a bridge with electron-donating property (D') with 1,4-dithiafulvene (DTF; TTF half unit) as a donor and dicyanomethylene (DCM; TCNE half unit) or an ethoxycarbonyl-cyanomethylene (ECM) as an acceptor were designed and synthesized. The pulse radiolysis study of **1a** in 1,2-dichloroethane allowed the clear assignment of the absorption bands of the DTF radical cation (**1a^{•+}**), while the absorption bands due to the DCM radical anion could not be observed by γ -ray radiolysis in 2-methyltetrahydrofuran rigid glass at 77K. Electrochemical oxidation of **1a** first generates the DTF radical cation (**1a^{•+}**), whose absorption bands are in agreement with those observed by the pulse radiolysis study, followed by dication (**1a²⁺**). The ESR spectrum of **1a^{•+}** showed a symmetrical signal with fine structure and ESR simulation predicted that the spin of **1a^{•+}** is delocalized over S and C atoms of

the DTF moiety and the central C atom of the trimethylene bridge bearing DTF moiety. Pulse radiolysis, ESR, and electrochemical studies indicate that the DTF radical cation of **1a^{•+}** is more stable than that of **6^{•+}**, and the latter shows strong tendency to dimerize. This result indicates that [3.3]PCP moiety as a bridge can stabilize the DTF radical cation more than 1,3-diphenylpropane moiety because of kinetic stability due to its rigid structure and the weak electronic interaction of DTF and DCM moieties through [3.3]PCP.

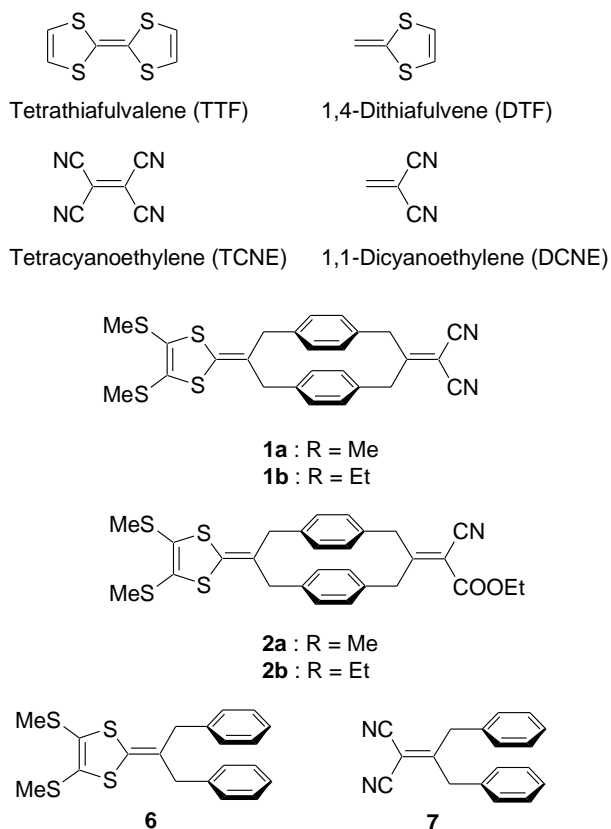
Introduction

Tetrathiafulvalene (TTF) is known as the strong electron donor (D) that possesses highly reversible oxidation states and is successfully used as a building block for organic conductors.^[1] Aviram and Ratner proposed the concept of the unimolecular rectifier based on the TTF(D)-bridge(B)-TCNQ(A) dyad with bicyclooctane as a rigid σ -bridge.^[2] Particularly, since their proposal, many TTF(D)-B-A dyads with a σ - or π -bridge have been synthesized. These dyads offer considerable potential to develop molecular electronics materials that applied intramolecular charge transfer (ICT) process between D and A.^[3-6] Molecular electronics as nonlinear optical (NLO) materials and display electrochromic materials are based on ICT process between D and A through bridges.^[7] As the stable charge separated state D⁺-B-A⁻ with fixed D⁺ and A⁻ distance and the electron tunneling between D and A are prerequisite for in TTF(D)-B-A molecular rectifier proposed by Aviram and Ratner, the development of intramolecular rectification electronics requires the D-B-A dyads with a rigid σ -bridge. In the past decades, flexible σ -bridges have been used in TTF(D)-B-A dyads so far,^[4] and there has been no report on those with a rigid σ -bridge (i.e. bicyclooctane) such as the Aviram-Ratner model^[2]. Recently, the Langmuir-Blodgett monolayer of TTF(D)-B-A dyads containing trinitrofluorene (A) were reported to be the a few examples of the molecular rectifier in many TTF(D)- σ (B)-A dyads.^[4a, 1]

1,4-Dithiafulvene (DTF; TTF half unit, 1,3-dithiole-2-ylidene) serves as an electron donating building block for diverse organic materials such as organic superconductors,^[8] and its radical cation has thermodynamic stability (Chart 1). In the reported DTF(D)-B-A dyads, π -spacers have been used as bridges mostly, and these dyads have been applied to dye-sensitized solar cells and nonlinear optical materials.^[9] In DTF(D)- σ (B)-DCM(A) dyads, only a few examples employed rigid σ -bridge.^[10]

- [a] Prof. Dr. K. Sako, T. Hasegawa, Y. Kato, H. Onda, Prof. Dr. M. Shiotsuka
Department of Life Science and Applied Chemistry
Nagoya Institute of Technology
Gokiso, Showa-ku, Nagoya 466-8555, Japan
E-mail: sako@nitech.ac.jp
- [b] Prof. Dr. M. Watanabe
International Institute for Carbon-Neutral Energy Research (I2CNER)
Kyushu University
744 Motoooka, Nishi-ku, Fukuoka, 819-0395 Japan
- [c] Prof. Dr. Teruo Shinmyozu
Department of Chemistry
National Taiwan University
No. 1, Section 4, Roosevelt Rd, Taipei, 10617, Taiwan
- [d] Dr. S. Tojo, Prof. Dr. M. Fujitsuka, Prof. Dr. T. Majima
The Institute of Scientific and Industrial Research (SANKEN)
Osaka University
Mihogaoka 8-1, Ibaraki, Osaka, 567-0047, Japan
- [e] Prof. Dr. Y. Hirao, Prof. Dr. T. Kubo
Department of Chemistry, Graduate School of Science
Osaka University
Machikaneyama 1-1, Toyonaka, Osaka 560-0043, Japan
- [f] Prof. Dr. T. Iwanaga
Department of Chemistry, Faculty of Science
Okayama University of Science
Ridaicho 1-1, Kita-ku, Okayama 700-0005, Japan
- [g] Prof. Dr. S. Toyota
Department of Chemistry, School of Science
Tokyo Institute of Technology
2-12-1, Ookayama, Meguro-ku, Tokyo 152-8550, Japan
- [h] Prof. Dr. H. Takemura
Department of Chemical and Biological Science, Faculty of Science
Japan Women's University
Mejirodai 2-8-1, Bunkyo-ku, Tokyo 112-8681, Japan

Supporting information for this article is given via a link at the end of the document.



28 **Chart 1.** Molecular structures of TTF, DTF, TCNE, DCM, the target molecules
29 (1, 2), and the reference compounds.

30
31
32 The use of [2.2]- or [3.3]PCP as a bridge can promote ICT
33 and control electronic interaction by the π - π stacking within
34 cyclophane.^[11] Thus, D-B(PCPs:D')-A triads are interesting
35 candidates for molecular electronics materials, and these D-A
36 systems based on PCPs can be classified into three types
37 according to the ways of introducing D and A into PCP as
38 follows (Chart 2); type A: the CT (D-A) cyclophanes, type B: the
39 cyclophanes substituted with D and A at the *pseudopara* positions,
40 type C: cyclophanes with D and A incorporated into the bridge
41 chains.

42 Over three decades, rigid two- to four-layered CT (D-A)
43 cyclophanes (type A) were synthesized by Staab's group,^[12]
44 Misumi's group,^[13] and Shinmyozu's group,^[14] and they were
45 used as model compounds for the clarifications of the
46 dependence of CT interaction on transannular distance and
47 relative orientation of A and D. In the past decade, there has
48 been a growing interest in the use of [2.2]- or [3.3]PCP as a
49 bridge in the D-B(PCP)-A triads (type B), in which D-
50 PCP([2.2]PCP or [3.3]PCPs)-A triads are expected to show
51 photoinduced charge separation phenomena with long lifetime,
52 and these triads have been applied as organic solar cell^[15] and
53 NLO materials.^[16]

54 On the other hand, there have been no reports of D-B(D')-A
55 triads (type C), where π -systems of A and D are orthogonal to
56 the benzene rings of the cyclophane, which is different from
57 spiro π -conjugation. As far as we know, there are a few

58
59
60
61
62
63
64
65

examples of D-B(D')-D triads and B(D)-A dyads^[17] which can be categorized as type C. Previously, we reported that electronic interaction between orthogonal arranged DTF and benzene rings of [3.3]PCP in D-B(D')-D triads.^[17e] We have expected that these triads show unique electronic interaction between D and A through cyclophane moiety to generate stable charge separated states.

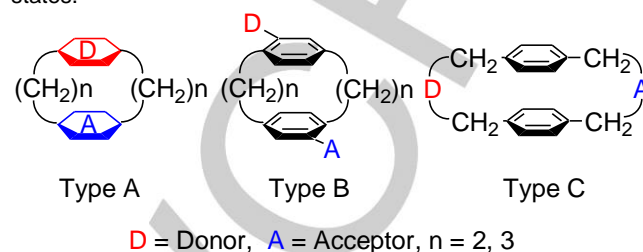


Chart 2. Three types of donor-cyclophane-acceptor triads.

Thus, we focused on a cylindrical and rigid structure of [3.3]PCP as a rigid spacer of D-B-A triads, instead of the bicyclooctane bridge, in order to construct the rigid triads with fix D-A distance (Chart 1). We synthesized DTF(D)-[3.3]PCP(B)-DCM or ECM (A) triads, in which [3.3]PCP was used as a σ -spacer with electron-donating property (D'). In this paper, we report the synthesis, structure, electrochemical and photophysical properties of the triads 1 and 2, and properties of the DTF radical cation **1a⁺** based on pulse radiolysis, electrochemical, and ESR studies.

Results and Discussion

Synthesis

The synthesis of DTF-[3.3]PCP-DCM triads **1a-b** and DTF-[3.3]PCP-ECM triads **2a-b** is shown in Scheme 1. The corresponding 1,3-dithiole phosphonate esters **3a-b**^[18] and [3.3]paracyclophane-2-11-dione **4**^[19] were prepared according to the literature procedures. Cyclophane **4** was reacted with the anion generated from phosphonate esters **3a-b** by *n*BuLi in dry THF at -78 °C, and the reaction mixture was slowly warmed up to room temperature. After the solvent was evaporated, the reaction mixture was purified by column chromatography on silica gel with CH_2Cl_2 /hexane (2/1) as an eluent to afford the triad precursor cyclophane monoketones **5a-b** in 47 and 57% yield, respectively. Then the cyclophanes **5a-b** were reacted with malononitrile or ethyl cyanoacetate in the presence of ammonium acetate and acetic acid in benzene at reflux. After removal of the solvents, the reaction mixture was purified by column chromatography on silica gel with CH_2Cl_2 as an eluent or recrystallization from CH_2Cl_2 -MeOH. The target triads **1a-b** and **2a-b** were obtained 84, 80, 87, and 60% yields, respectively. All compounds synthesized were fully characterized by ¹H-NMR, ¹³C-NMR, IR, and MS data.

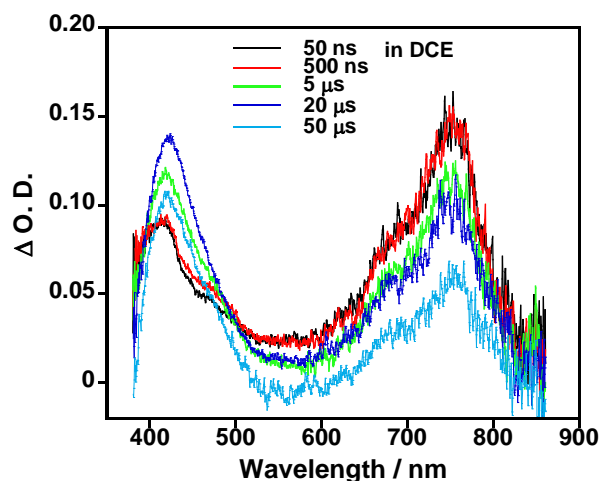


Figure 3. Transient absorption spectra observed at 50, 500 ns and 5, 20, 50 μ s after an electron pulse the triad **1a** (2.5mM) in DCE under Ar atmosphere at 295 K.

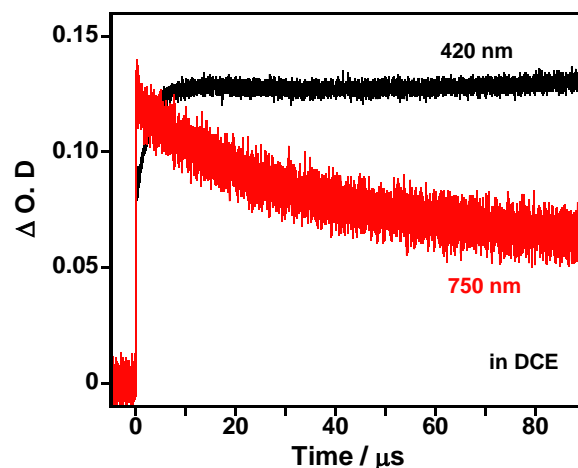
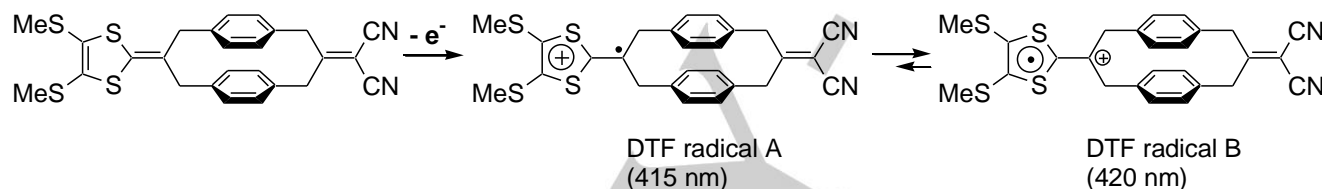


Figure 4. Kinetic traces of Δ O.D. at 420 and 750 nm during the pulse radiolysis of the triad **1a** (2.5 mM) in DCE under Ar atmosphere at 295K.



Scheme 2. Possible DTF radical cations of the triad **1a**.

The intensity of the bands at 677 and 750 nm gradually decreased and shifted to the longer wavelength region by ca. 10 nm until 50 μ s. On the other hand, the intensity of the band in the region of 400 – 500 nm gradually increased up to 50 μ s and shifted to 420 nm. The absorption spectrum at 50 ns after an electron pulse can be assigned to the first generated DTF radical cation **1a**^{•+} (DTF radical A) [λ_{max} : 415, 467 (sh), 677 (sh), and 750 nm], and the new band at 420 nm at 20 μ s after an electron pulse is due to another structure of the DTF radical cation **1a**^{•+} (DTF radical B) (Scheme 2).^[20] Because of the presence of intramolecular electronic interaction between the DTF and benzene rings of [3.3]PCP in the ground state, positive charge of DTF radical cation would be partly located on [3.3]PCP. The radical cation of bis(benzyl)DTF **6** [λ_{max} : 414, 467 (sh), 676 (sh), and 750 nm] exhibited similar transient absorption bands to those of **1a** at 415 and 750 nm as well as the shoulders at ca. 467 and 677 nm (Figure 5S). Although the intensity of the bands at 676 and 750 nm in **6**^{•+} gradually decreased, these bands as well as the band at 414 nm did not shift to the longer wavelength region.

The time profiles of **1a** and **6** at 420 (415) and 750 nm during the pulse radiolysis are shown in Figure 4, Figure 6S, and Table 1. The decay profiles of **1a** and **6** monitored at 750 nm showed multicomponent decay up to 90 μ s, indicating the presence of the components with shorter and longer time decays. The time decay constants of **1a** and **6** were evaluated as τ_1 (**1a**: 16.5 μ s, **6**: 4.4 μ s) and τ_2 (**1a**: 82.8 μ s, **6**: 34.7 μ s). As

Table 1. The decay lifetimes of the triad **1a** and the related compound **6** at 750nm and 420 or 415 nm.

Compound	τ_1 (μ S) ^[a]	τ_2 (μ S) ^[a]	τ (μ S) ^[b]
1a	16.5	82.8	>90
6	4.4	34.7	33.4

[a] The decay lifetimes at 750 nm were measured in in DCE under Ar atmosphere at 295 K and double exponential decay fitting (eqn (1)) was used. [b] The decay lifetimes at 420 or 415 nm were measured in in DCE under Ar atmosphere at 295 K and single exponential decay fitting (eqn (2)) was used.

$$\Delta OD = A_1 \exp\left[-\frac{(t-t_0)}{\tau_1}\right] + A_2 \exp\left[-\frac{(t-t_0)}{\tau_2}\right] + A_{\text{off}} \quad (1)$$

$$\Delta OD = A_1 \exp\left[-\frac{(t-t_0)}{\tau_1}\right] + A_{\text{off}} \quad (2)$$

shown in Figure 4, the decay rate of the DTF radical B observed at 420 nm is faster than the decay rate of the DTF radical A, and the concentration of the DTF radical B is constant after 10 μ s, while the concentration of the DTF radical A is decreased even after 10 μ s. These data indicate that the first generated DTF radical cation (DTF radical A) converts to another structure of

the DTF radical cation (DTF radical B) under the pulse radiolysis conditions (Figure 4 and Scheme 2). Different from the time profile of **1a**, the concentration of the DTF radical cation of **6** (415 nm) is decreased even after 80 μ s, indicating its instability compared to that of **1a^{•+}** (Figure 6S). Clearly, the lifetime of the DTF radical cation of **1a** is longer than that of the bis(benzyl)DTF **6**, indicating that the DTF radical cation is stabilized by rigid structure of [3.3]PCP. The absorption spectrum of **1a** in 2-methyltetrahydrofuran (MTHF) rigid glass at 77K after γ -radiolysis is similar to that of **1a** at 50 ns after an electron pulse (Figure 3S and Figure 4S), but the absorption band due to the DCM radical anion was not observed.

Electrochemical properties

In order to study the electrochemical properties of **1a-b** and **2a-b**, cyclic voltammograms and differential pulse voltammograms of **1** and **2** were measured in CH_2Cl_2 (Figure 5, ESI†). The redox potentials of **1** and **2** are summarized in Table 2 along with those of the references, bis(benzyl)DTF **6** and bis(benzyl)DCM **7**. The first and second oxidation processes of **1** and **2** (E_{ox1} : +0.32 to +0.34 V, E_{ox2} : +0.73 to +0.74 V, V vs. Fc/Fc⁺) correspond to the formation of the radical cation and dication of the DTF moiety (Scheme 1S), respectively, based on the pulse radiolysis study as described above. The first oxidation potentials (E_{ox1} : +0.32 to +0.34 V) of **1** and **2** are slightly higher than that of **6** (E_{ox1} : +0.30V; Figure 14S). This result suggests that weak intramolecular electronic interaction between DTF donor and

[3.3]PCP is present, and positive charge of the DTF radical cation would be mostly localized over the 1,3-dithiole ring. The

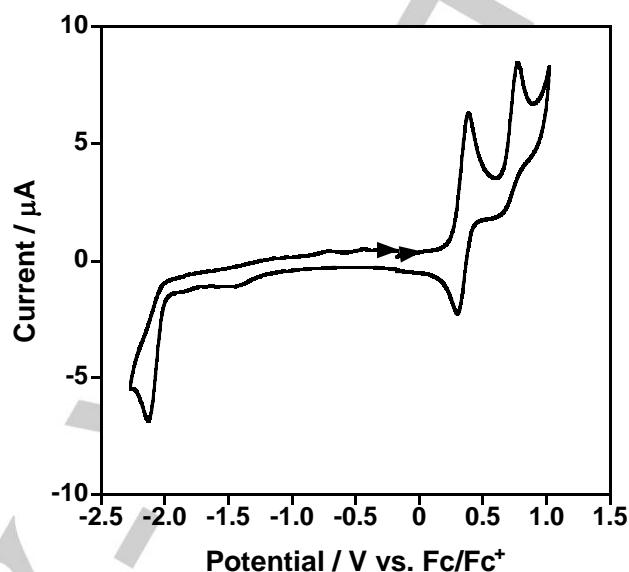


Figure 5. Cyclic voltammogram of **1a** under the conditions (in $\text{CH}_2\text{Cl}_2/0.1\text{M}$ $n\text{Bu}_4\text{NPF}_6$, Ag/AgNO₃ as the reference electrode, Pt as the working and counter electrode at the potential scan rate of 0.1V/s. Potentials are referred to vs. Fc/Fc⁺(V)).

Table 2. Electrochemical data of triads **1**, **2**, and the related compounds.

Compound	$E_{\text{ox1}} / [\text{V}]^{\text{[a]}}$	$E_{\text{ox2}} / [\text{V}]^{\text{[a]}}$	$E_{\text{ox3}} / [\text{V}]^{\text{[b][c]}}$	$E_{\text{red}} / [\text{V}]^{\text{[b][d]}}$	HOMO / [eV] ^[e]	HOMO / [eV] ^[f]	LUMO / [eV] ^[e]	LUMO / [eV] ^[f]	$E_g^{\text{exp}[g]}$
1a	+0.34	+0.74	+1.45	-2.12	-5.35	-5.41	-3.16	-2.29	2.19
1b	+0.33	+0.75	+1.46	-2.12	-5.36	-5.35	-3.15	-2.28	2.21
2a	+0.32	+0.73	+1.36	-2.28	-5.34	-5.26	-3.03	-1.95	2.31
2b	+0.34	+0.74	+1.38	-2.26	-5.36	-5.20	-3.06	-1.94	2.30
5a	+0.32	+0.72	+1.40		-5.35				
5b	+0.33	+0.73	+1.39		-5.35				
6	+0.30	+0.74			-5.32				
7				-2.15			-3.15		

[a] Determined from the cyclic voltammograms in $\text{CH}_2\text{Cl}_2/0.1\text{M}$ $n\text{Bu}_4\text{NPF}_6$, Ag/AgNO₃ as the reference electrode, Pt as the working and counter electrode at the potential scan rate of 0.1V/s. Potentials are referred to vs. Fc/Fc⁺(V), reversible step. [b] irreversible step. [c] E_{ox3} is anodic peak potential. [d] E_{red} is cathodic peak potential. [e] HOMO = - ($E_{\text{pa}}^{\text{onset}} + 5.1$) and LUMO = - ($E_{\text{pc}}^{\text{onset}} + 5.1$). [f] HOMO and LUMO are estimated by DFT methods (B3LYP/6-31G* level). [g] E_g^{exp} = HOMO - LUMO.

third oxidation potentials of **1** and **2** (E_{ox3} : +1.36 to +1.46 V), which are assigned to one electron oxidation of [3.3]PCP moiety to its cation radical species, are higher than that of [3.3]PCPs (E_{ox} : +1.07 V).^[21] Probably, this anodic shift is due to an introduction of A and D into the central carbon of the trimethylene bridges and electrostatic repulsion from the dication species of the DTF moiety. Thus, [3.3]PCP serves as a bridge with electron-donating properties (D'). The reduction process of **1a** (E_{red} : -2.12 V), **1b** (E_{red} : -2.12 V) or **2a** (E_{red} : -2.26 V), and **2b** (E_{red} : -2.28 V) can be attributed to the formation of the radical anion species of DCM or ECM moiety, respectively. As the electron accepting ability of ECM substitute was weaker than that of DCM substitute,^[10] the reduction potentials of **2** are lower than that of **1**. The reduction potentials (E_{red} : -2.12 V) of **1a** and **1b** are slightly lower than that of the bis(benzyl)DCM **7** (E_{red} : -2.15 V; Figure 15S), and this suggests the presence of intramolecular electronic interaction between DCM and [3.3]PCP.

The presence of a weak electronic interaction between D and A through B([3.3]PCP) is further suggested by DFT (B3LYP/6-31G*) theoretical calculations using GAUSSIAN 09 (Figure 6).^[22] The HOMO and LUMO energies were also estimated by experimental redox potentials^[23] and theoretical calculations (Table 2 and Figure 6), which indicate that HOMO energies of **1a-b** and **2a-b** are almost same as those of the DTF-[3.3]PCP-one **5** and bis(benzyl)DTF **6**. The trends of theoretically estimated HOMO and LUMO energies are well agreed with experimental data of cyclic voltammogram values. The LUMO orbitals of **1a** and **2a** are mostly localized over DCM and ECM, respectively, and partly over the benzene rings of the [3.3]PCP and the trimethylene bridge bearing the DCM or ECM

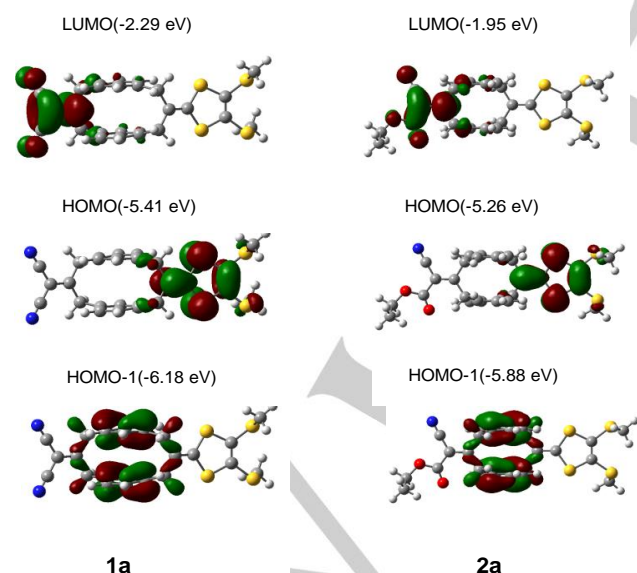


Figure 6. Molecular orbitals of the triads **1a** and **2a** calculated by the DFT method at the B3LYP/6-31G* level.^[22]

moiety, while the HOMO orbitals are mostly localized over the DTF moiety and partly over the trimethylene bridge bearing DTF moiety and the benzene rings of [3.3]PCP. The HOMO-1 orbitals are completely localized over the cyclophane moiety (Figure 6). These results show that the positive charge of the radical cation species of the triads **1a** and **2a** predominantly present on the DTF ring and partly on the benzene rings and the trimethylene bridge bearing the DTF moiety. These results indicate the presence of indirect weak orbital interaction between DTF and DCM or ECM through [3.3]PCP in the ground state.

Stability and characterization of the radical cation species

Spectroelectrochemistry

Figure 7 shows absorption spectra of **1a** in CH_2Cl_2 recorded by applying potential ranging from 0 to +1.25 V. At the potential of +0.8 V, **1a** exhibits three λ_{max} 's at 415, 676 (sh), and 750 nm and shoulders at around 367 and 466 nm, which are quite similar to those of the radical cation **1a^{•+}** generated by pulse radiolysis (Figure 7). The bis(benzyl)DTF **6** also shows the λ_{max} 's at 413, 676 (sh), and 750 nm at a potential of +0.8 V and these bands are assigned to those of the DTF radical cation **6^{•+}** (Figure 8). The bands at 415, 676, and 750 nm of **1a** were found from TD-DFT calculation of **1a^{•+}** to be assigned to the DTF radical cation (Table 1S, Figure 16S, and Figure 17S). The band at 415 nm, which is assigned to the excited transitions of DTF radical cation and DTF radical cation-[3.3]PCP, corresponded with the λ_{max} at 380 nm obtained by TD-DFT calculations ($110\beta \rightarrow 128\beta$, $126\alpha \rightarrow 130\alpha$). The bands at 676 and 750 nm can be assigned to the excited transition of DTF radical cation-[3.3]PCP (TD-DFT; λ_{max} 626 nm, $122\beta \rightarrow 128\beta$) and that of **1a^{•+}** molecule – DTF radical cation (TD-DFT; λ_{max} 712 nm, $124\beta \rightarrow 128\beta$), respectively.

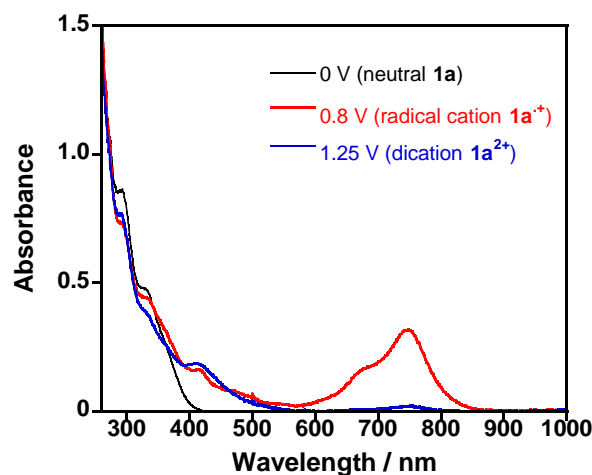


Figure 7. Absorption spectra of **1a** in CH_2Cl_2 (0.1M $n\text{Bu}_4\text{NPF}_6$) under the potential voltages of 0, 0.8, and 1.25 V vs. Ag/Ag^+ .

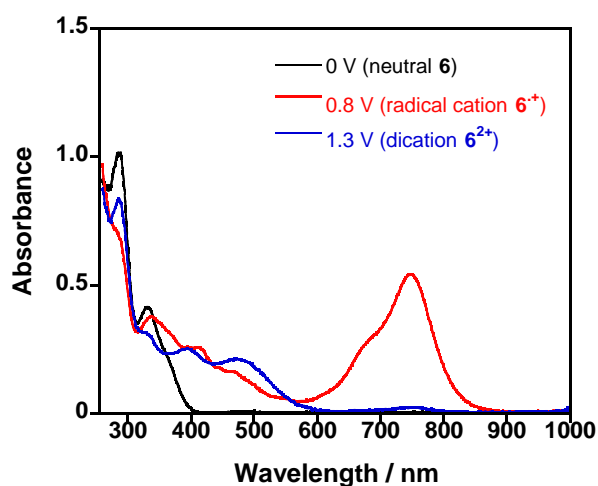
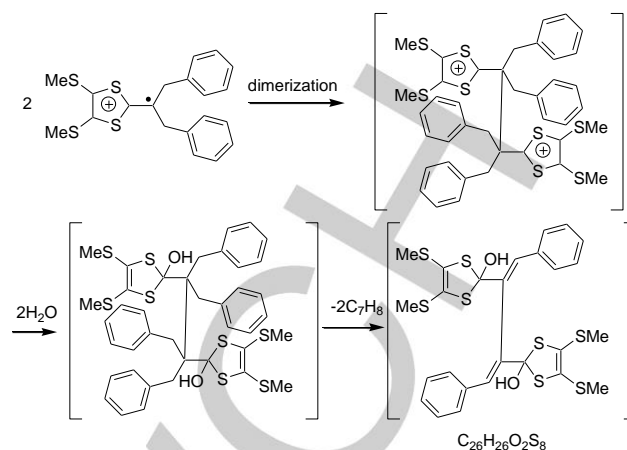


Figure 8. Absorption spectra of **6** in CH_2Cl_2 (0.1M $n\text{Bu}_4\text{NPF}_6$) under the potential voltages of 0, 0.8, and 1.3 V vs. Ag/Ag^+ .

At more positive potential of +1.25 V, the absorption bands at 676 and 755 nm disappeared, while the absorption intensity of the band at 411 nm increased, and this significant spectral change is assigned to the generation of the DTF dication $1\mathbf{a}^{2+}$ from the radical anion $1\mathbf{a}^{\bullet-}$. The related DTF diphenylpropane compound (**6**) also showed similar absorption bands at 340, 413, 466(sh), 676(sh), and 751 nm at a potential of +0.8 V by DTF radical cation formation (Figure 8). DTF diphenylpropane **6** showed two new bands at 395 and 473 nm and the long wavelength bands at 676 and 751 nm disappeared at potential of +1.3 V. The bis(benzy)DTF **6** also showed similar spectral changes at the potential of +1.3 V, indicating the generation of the dication 6^{2+} (Figure 8). After electrochemical oxidation of **6** at +0.8 V for 5 min, however, the new intense λ_{max} 's appeared at 397 and 475 nm, which are different from the band due to the radical cation species of $6^{\bullet+}$, along with the λ_{max} 's at 676 (sh) and 755 nm due to the DTF radical cation (Figure 18S). As these new observed bands at 397 and 475 nm are similar to those of the dication 6^{2+} , this result suggests that the dication 6^{2+} species were generated by disproportionation or dimerization of $6^{\bullet+}$ species under electrochemical oxidation at +0.8 V for 5 min. FAB-MS spectrum of the solution showed two main molecular ion peaks at m/z 388.048 (M^+ , calcd. 388.045) that corresponds to the neutral reference **6** ($\text{C}_{20}\text{H}_{20}\text{S}_4$) and at m/z 629.551 ($(M-H)^+$, calcd. 629.001), which might correspond to the signal of the neutral dimer derivative obtained from the dimer dication 6^{2+} via $6^{\bullet+}$ (Scheme 3, Figure 19S, and Figure 20S).^[24]

In contrast, the absorption bands of the DTF radical cation species $1\mathbf{a}^{\bullet+}$, which were generated by electrochemical oxidation at +0.8 V for 5 min, were intact (Figure 21S). These results indicate that the DTF radical cation $1\mathbf{a}^{\bullet+}$ is more stable than the radical cation $6^{\bullet+}$ under the conditions and the radical cation $6^{\bullet+}$ tends to dimerize, probably because of the kinetic stability of $1\mathbf{a}^{\bullet+}$ by steric hindrance of the rigid [3.3]PCP structure and the presence of weak electronic interaction between DTF and DCM moieties through [3.3]PCP.



Scheme 3. Dimerization mechanism of DTF reference **6** under electrochemical oxidation conditions.

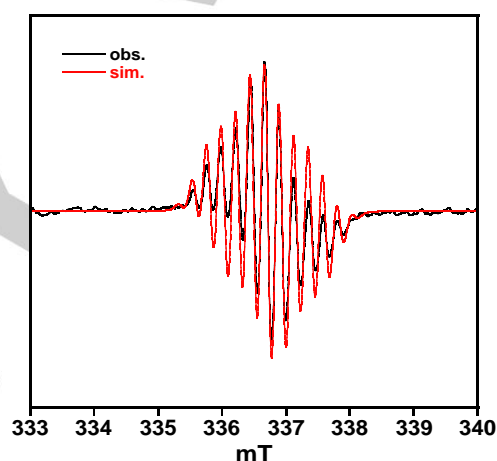


Figure 9. ESR spectrum of **1a** (1mM) in CH_2Cl_2 (0.1 M $n\text{Bu}_4\text{NPF}_6$); +0.8 V. Ag/Ag^+ .

ESR study

In order to characterize the DTF radical cation $1\mathbf{a}^{\bullet+}$, ESR spectrum of the electrochemically oxidized species of **1a** in CH_2Cl_2 at a potential of +0.8 V (vs. Ag/Ag^+) was measured. The observed ESR shows a symmetrical signal with fine structure (Figure 9), and agreed with simulated ESR spectra of **1a**. The ESR signal of **1a** consists of eleven lines with g -value of 2.0072 and two coupling constants of $a(6\text{H}) = 0.22$ mT and $a(2\text{H}) = 0.68$ mT. The hyper interactions between six hydrogen atoms of methylthio groups and two benzylic hydrogen atoms of the trimethylene bridge were considered, since six methyl hydrogens are equivalent by the rapid rotation of the methylthio group and four benzylic hydrogens are non-equivalent by slow conversion of the trimethylene bridge. Based on the DFT calculations (UB3LYP/6-31G), the spin distribution is delocalized over four sulfur atoms and two sp^2 carbons of 4,5-bis(methylthio)-1,3-dithiole-2-ylidene moiety, and the central

1 carbon atom of the trimethylene bridge bearing the DTF moiety
2 (Figure 22S).

3 In contrast, the ESR spectrum of the radical cation $6^{+\bullet}$,
4 which was generated by the same electrochemical oxidation at
5 +0.8 V, is not symmetric and this indicates the presence of two
6 or more different radical cation species (Figure 23S). Thus, the
7 instability of the radical cation $6^{+\bullet}$ compared to that of $1^{+\bullet}$ was
8 again demonstrated by the ESR study. By introducing rigid
9 [3.3]PCP as B and D' in between DTF(D) and DCM(A), the DTF
10 radical cation could be kinetically stabilized.

11 Molecular structure and spin distribution of $1a$ were
12 calculated on the basis of the DFT methods (UB3LYP/6-31G*)
13 GAUSSIAN 09 Package (Figure 22S).^[22] There are two possible
14 conformations of the radical cation of $1a$, namely the parallel and
15 orthogonal conformations by relations between 1,3-dithiole ring
16 and benzene rings of [3.3]PCP. The orthogonal conformation is
17 defined that the 1,3-dithiole ring lies orthogonal to the benzene
18 rings of [3.3]PCP, whereas the parallel one denotes parallel to
19 the benzene rings of [3.3]PCP. The optimized molecular
20 structure of $1a^{+\bullet}$ has the orthogonal conformation (Figure 24S),
21 similar to the structure of neutral $1a$.

22 Conclusions

23
24
25 The new triads, DTF(D)-[3.3]PCP(D')-DCM or ECM **1** and **2**, in
26 which the DTF and DCM moieties are orthogonal to the benzene
27 rings of [3.3]PCP were synthesized and their structures were
28 elucidated by single crystal X-ray analysis and DFT theoretical
29 calculations. One electron oxidized species of $1a$, the radical
30 cation $1a^{+\bullet}$, was generated by pulse radiolysis and the first
31 generated radical cation $1a^{+\bullet}$ converts to another structural
32 radical cation species $1a^{2+\bullet}$ in 50 μ s after an electron pulse. The
33 $1a^{+\bullet}$ and $1a^{2+\bullet}$ species are generated by stepwise electrochemical
34 oxidation processes, and $1a^{+\bullet}$ was found to be more stable than
35 that of the bis(benzyl)DTF $6^{+\bullet}$, which shows tendency to dimerize.
36 ESR spectral study indicates the homogeneity of $1a^{+\bullet}$, whereas
37 the ESR signal of $6^{+\bullet}$ contains a few radical species. The ESR
38 study indicated that the stability of $1a^{+\bullet}$ is ascribed to
39 delocalization of spin on four sulfur and two carbon atoms in the
40 1,3-dithiole ring and the central carbon atom of the [3.3]PCP
41 trimethylene bridge. The electrochemical, and molecular orbital
42 studies indicate the presence of weak electronic interaction
43 between DTF and DCM moieties through [3.3]PCP. Thus, the
44 higher stability of $1a^{+\bullet}$ compared to $6^{+\bullet}$ is ascribed to this weak
45 electronic interaction, kinetic stability by steric hindrance and
46 rigid cyclophane structure that prohibit dimerization of the DTF
47 radical cation. The D-B(D')-A triads **1** and **2** can stabilize the
48 DTF radical cation by introduction of rigid [3.3]cyclophane
49 without substitution of sterically bulky substituents into the DTF
50 radical cation and [3.3]PCP in these DTF-[3.3]PCP-A triads can
51 be functioned as a rigid σ -bridge. These new D-B(D')-A triads
52 offer potential opportunity for the design of new molecular
53 rectifier model and orthogonal π -systems different from spiro π -
54 conjugation.

Experimental Section

General

All dry solvents were distilled by standard procedures (THF from Na/benzophenone under N_2 , benzene from CaH_2 under N_2). The other chemicals were obtained commercially and used without further purification. Moisture-sensitive reactions were carried under an argon atmosphere. NMR spectra were recorded on JEOL AL-300 nuclear magnetic resonance spectrometer (300 MHz for 1H and 75MHz for ^{13}C NMR). Chemical shifts are reported downfield from TMS, referenced to the chloroform-d solvent. Infrared spectra were measured on a JASCO FT/IR-460 plus. High resolution mass spectrometry was performed with a JEOL MSatation-700. Melting points are uncorrected and were obtained on a Mel-Temp apparatus.

Synthesis

Compound 5a. In a two necked flask, to a solution of the phosphonate **3a** (61 mg, 0.20 mmol) in dry THF (8 mL) at $-78^\circ C$ under Ar atmosphere, *n*BuLi (0.16 mL, 0.24 mmol, 1.6 M) was slowly added dropwise. The mixture was stirred at $-78^\circ C$ for 20 min, while the mixture was turned into a red solution. Then, a solution of [3.3]paracyclophane-2,11-dione **4** (53 mg, 0.20 mmol) in dry THF (16 mL) was slowly added to the reaction mixture. After stirring for 1 h at $-78^\circ C$, the mixture was allowed slowly to warm to the room temperature and stand overnight. The solvent was removed under vacuum, water (15 mL) was added to the residue and obtained pale pink solid by filtration and washing with methanol. The resulting pale pink solid was purified by column chromatography on silica gel (eluents dichloromethane/*n*-hexane 2:1) to afford **5a** as a pale pink solid (47 mg, 47%). M.p. 206-208 $^\circ C$; 1H NMR (300 MHz, $CDCl_3$) δ 2.46 (s, 6H), 3.40 (s, 4H), 3.68 (s, 4H), 6.75 (s, 8H); ^{13}C NMR (75 MHz, $CDCl_3$) δ 18.8, 43.2, 51.9, 125.3, 126.8, 130.3, 133.7, 137.6, 137.6, 207.3; IR (KBr disk) ν (cm^{-1}) 804, 823, 837, 866, 890, 1109, 1428, 1509, 1631, 1687, 2851, 2919, 2952, 2991, 3016; FAB-HRMS m/z calcd. for $C_{23}H_{24}OS_4$: 442.0554; found: 442.0537 [M^+].

Compound 5b. Compound **5b** was obtained by the method similar to the preparation of **5a** using **3b** instead of **3a** as pale pink solid (yield: 58%). M.p. 142-144 $^\circ C$; 1H NMR (300 MHz, $CDCl_3$) δ 1.37 (t, $J = 7.3$ Hz, 6H), 2.89 (q, $J = 7.3$ Hz, 4H), 3.40 (s, 4H), 3.68 (s, 4H), 6.75 (s, 8H); ^{13}C NMR (75 MHz, $CDCl_3$) δ 15.1, 30.1, 43.2, 51.9, 125.0, 125.7, 129.8, 130.3, 133.6, 137.6, 207.3; IR (KBr disk) ν (cm^{-1}) 808, 824, 866, 1084, 1109, 1239, 1257 1430, 1509, 1630, 1691, 2853, 2921, 2955, 2999, 3022; FAB-HRMS m/z calcd. for $C_{25}H_{26}OS_4$: 470.0867; found: 470.0875 [M^+].

Compound 1a. In a flask was placed **5a** (37 mg, 0.080 mmol), malononitrile (170 mg, 2.6 mmol) and ammonium acetate (420 mg, 5.4 mmol) in a mixed solvent of benzene (17 mL) and glacial acetic acid (3 mL). The flask was equipped with a Dean-Stark apparatus, the mixture was stirred for 48h under reflux. After cooling to room temperature, the reaction mixture was diluted with water (10 mL), and extracted with CH_2Cl_2 (15 mL X3). The combined organic layer was washed with water (15 mL X3), dried over $MgSO_4$, and the solvent was removed under vacuum. The resulting yellow residue was purified with by column chromatography on silica gel (eluents dichloromethane) to afford **1a** as a pale yellow solid (37 mg, 90%). M.p. 230-232 $^\circ C$; 1H NMR (300 MHz, $CDCl_3$) δ 2.46 (s, 6H), 3.40 (s, 4H), 3.90 (s, 4H), 6.72 (dd, $J_1 = 8.2$ Hz, $J_2 = 23.1$ Hz, 8H); ^{13}C NMR (75 MHz, $CDCl_3$) δ 18.8, 43.1, 43.5, 88.1, 112.2, 124.9, 125.4, 127.4, 130.1, 130.2, 133.4, 138.4, 182.0; IR (KBr disk) ν (cm^{-1}) 802, 834, 889, 1109, 1185, 1260, 1384, 1419, 1432, 1508, 1572, 1587, 1606, 2230, 2852, 2921, 2959,

2998, 3018; FAB-HRMS m/z calcd. for $C_{26}H_{22}N_2S_4$: 490.0666; found: 490.0698 [M^+].

Compound 1b. Compound **1b** was obtained by the method similar to the preparation of **1a** using **5b** instead of **5a** as a pale yellow solid (yield: 80%). M.p. 174–176 °C; 1H NMR (300 MHz, $CDCl_3$) δ 1.35–1.40 (m, 6H), 2.85–2.93 (m, 4H), 3.40 (s, 4H), 3.89 (s, 4H), 6.72 (dd, $J_1 = 7.9$ Hz, $J_2 = 22.6$ Hz, 8H); ^{13}C NMR (75 MHz, $CDCl_3$) δ 15.1, 30.1, 43.0, 43.6, 88.1, 112.2, 123.6, 124.5, 124.6, 125.8, 127.5, 127.6, 130.1, 130.2, 133.4, 138.4, 182.0; IR (KBr disk) ν (cm^{-1}) 802, 836, 889, 1054, 1112, 1189, 1260, 1419, 1436, 1507, 1571, 1586, 1605, 2230, 2852, 2920, 2962, 2997, 3019; FAB-HRMS m/z calcd. for $C_{26}H_{22}N_2S_4$: 518.0979; found: 518.0994 [M^+].

Compound 2a. Compound **2a** was obtained by the method similar to the preparation of **1a** using ethyl cyanoacetate instead of malononitrile as pale pink solid (yield: 87%). M.p. 185–187 °C; 1H NMR (300 MHz, $CDCl_3$) δ 1.41 (t, $J = 7.2$ Hz, 3H), 2.45 (s, 6H), 3.38 (s, 4H), 3.90 (s, 2H), 4.12 (s, 2H), 4.38 (dd, $J_1 = 7.1$ Hz, $J_2 = 14.3$ Hz, 2H), 6.65–6.76 (m, 8H); ^{13}C NMR (75 MHz, $CDCl_3$) δ 14.1, 18.8, 40.3, 43.1, 43.2, 46.1, 62.4, 107.7, 116.1, 125.2, 125.5, 125.6, 126.8, 129.8, 130.0, 130.1, 130.4, 134.5, 135.5, 137.1, 137.8, 161.9, 175.3; IR (KBr disk) ν (cm^{-1}) 773, 799, 892, 1028, 1083, 1113, 1186, 1231, 1273, 1439, 1508, 1592, 1619, 1730, 2221, 2852, 2922, 2961, 2977, 3016; FAB-HRMS m/z calcd. for $C_{28}H_{27}O_2NS_4$: 537.0925; found: 537.0955 [M^+].

Compound 2b. Compound **2b** was obtained by the method similar to the preparation of **1b** using ethyl cyanoacetate instead of malononitrile as pale pink solid (yield: 60%). M.p. 134–135 °C; 1H NMR (300 MHz, $CDCl_3$) δ 1.35–1.44 (m, 9H), 2.85–2.92 (m, 4H), 3.38 (s, 4H), 3.90 (s, 2H), 4.12 (s, 2H), 4.38 (dd, $J_1 = 7.1$ Hz, $J_2 = 14.3$ Hz, 2H), 6.65–6.76 (m, 8H); ^{13}C NMR (75 MHz, $CDCl_3$) δ 14.1, 15.1, 30.1, 40.3, 43.1, 43.2, 46.1, 62.4, 107.7, 116.1, 125.2, 125.4, 125.8, 126.9, 127.0, 127.5, 129.8, 130.0, 130.1, 130.4, 134.4, 135.5, 137.9, 161.9, 175.3; IR (KBr disk) ν (cm^{-1}) 775, 800, 893, 1027, 1085, 1112, 1189, 1232, 1274, 1418, 1442, 1508, 1589, 1605, 1728, 2220, 2834, 2868, 2922, 2979, 3020; FAB-HRMS m/z calcd. for $C_{30}H_{31}O_2NS_4$: 565.1238; found: 565.1243 [M^+].

X-ray crystallography

X-ray diffraction data were collected on a Rigaku VariMax with Saturn diffractometer for **1a** with Mo $K\alpha$ radiation ($\lambda = 0.71070$ Å) to a maximum 2θ value of 55.0°. All computations were performed using Yadokari-XG 2009 program.^[25] The structures were solved by the direct method (SHELXS-97) and refined by the full-matrix least-squares method. Non-hydrogen atoms were refined anisotropically. Some hydrogen atoms were refined using the riding model. Additional crystallographic data are as follows. **1a**: dimension $0.33 \times 0.09 \times 0.09$ mm³, formula $C_{26}H_{22}N_2S_4$, $M = 490.70$, monoclinic, space group $P2_1/c$ (No. 14), $a = 14.503(6)$, $b = 21.263(9)$, $c = 21.263(9)$ Å, $\beta = 99.405(6)^\circ$, $V = 2343.2(17)$ Å³, $Z = 4$, $D_c = 1.391$ g cm⁻³, μ (Mo $K\alpha$) = 0.423 mm⁻¹, $T = 120(2)$ K, $F(000) = 2000$, 5340 reflections, $R_1 = 0.0843$ ($I > 2.0\sigma(I)$), $wR_2 = 0.2426$. GOF 1.097. Crystallographic data reported in this manuscript have been deposited with Cambridge Crystallographic Data Centre as supplementary publication no. CCDC-1463789. Copies of the data can be obtained free of charge via www.ccdc.cam.ac.uk/conts/retrieving.html (or from the Cambridge Crystallographic Data Centre, 12, Union Road, Cambridge, CB2 1EZ, UK; fax: +44 1223 336033; or deposit@ccdc.cam.ac.uk).

Cyclic voltammetry

Cyclic voltammetry experiments have been carried at room temperature with a BAS ALS6105 B electrochemical analyzer, in a three-electrode cell

(Ag/Ag⁺ reference) using Pt disk (1.6 mm diameter) as a working electrode and Pt wire as a counter electrode. 0.1 M *n*Bu₄NPF₆ in CH₂Cl₂ was used as the electrolyte. All the potentials (except in the spectroelectrochemical section) are quoted vs. the ferrocene/ferrocenium (Fc/Fc⁺) couple.

Spectroelectrochemistry

Spectroelectrochemical data were recorded for compounds **1a** and **6** (ca. 10⁻⁴ M) in CH₂Cl₂ with *n*Bu₄NPF₆ (0.1 M) as supporting electrolyte on an Ocean Optics SD 2000 fiber optic spectrophotometer between 200 – 1100 nm at ambient temperature. Spectra were corrected for background absorption arising from the cell, the electrolyte and the working electrode. The optical thin-layer electrochemical cell used a Pt mesh working electrode, Pt wire counter and Ag/Ag⁺ reference electrodes. The solutions were analyzed in situ: the working electrode was held at a potential at which no electrochemical work was being done in the cell and the spectrum of the neutral compound was recorded, which was identical to the spectrum recorded for open-circuit conditions. The potential was then increased in 50 ± 700 mV increments and held until equilibrium had been obtained, as evidenced by a sharp drop in the cell current. The cell used can be operated either under semi-infinite diffusion or thin-layer conditions.

Pulse-radiolysis and γ -radiolysis

Pulse radiolysis experiments were performed using an electron pulse (28 MeV, 8 ns, 0.7 kGy/pulse) from a linear accelerator at Osaka University. The probe light from 450 W Xe-lamp (Ushio, UXL-451-0) was detected with a multichannel spectrometer (Hamamatsu Photonics, S3904-1024F). In the present pulse radiolysis study, the sample (2.5 mM typically) was dissolved in 1,2-dichloroethane (DCE) or DMF in order to generate radical cation or radical anion of the sample, respectively. The kinetic traces were measured by using a photomultiplier (Hamamatsu Photonics, R2949). The sample for γ -ray radiolysis (1 mM typically) was dissolved in *n*-butyl chloride (BuCl) or 2-methyltetrahydrofuran (MTHF) to generate radical cation or radical anion, respectively. After the several freeze-pump-thaw cycles of the sample solution in a quartz cell (2 mm of optical path), the sample was kept at 77 K to form transparent glass, and then subjected to γ -ray irradiation (a ⁶⁰Co γ source: total dose, 1.54 kGy). The absorption spectra of the γ -ray irradiated sample at 77 K were measured using Shimadzu UV-3100.

ESR

The ESR measurements were carried out by using an electrochemical ESR based on a JEOL JES-FA200 spectrometer equipped a field frequency (F/F) lock accessory and a built in NMR gaussmeter. The electrochemical experiments were performed by in situ electrochemical oxidation using ALS 2323 bi-potentiostat. The electrochemistry experiments have been used on an ESR cell equipped with Pt wires as working and counter electrodes and Ag/Ag⁺ reference electrodes. Other experimental conditions were similar to spectroelectrochemistry experimental conditions.

Molecular orbital calculations

Optimized structures and electron densities of the neutral cyclophane triads and radical cation were estimated at the B3LYP/6-31G(d) level using GAUSSIAN 09 package. The optimized structures are confirmed to be the equilibrated most stable ones from the absence of imaginary frequencies.

Acknowledgements

We thank Dr. Hiroshi Ebisu for the ESR measurement supporting at Nagoya Institute of Technology. K.S. gratefully acknowledges the financial support for a Grant-in-Aid for Scientific Research (C) (No. 16550030, 16K05693) and Network Joint Research Center for Materials and Devices..

Keywords: paracyclophane • triad • donor-acceptor system • dithiafulvene • radical cation

- [1] a) *TTF Chemistry: Fundamentals and Applications and Tetrathiafulvalene* (Ed.: J.-i. Yamada, T. Sugimoto), Springer, New York, **2004**; b) M. R. Bryce, *J. Mater. Chem.* **2001**, *10*, 589–598; c) J. Segura, N. Martin, *Angew. Chem. Int. Ed.* **2001**, *40*, 1372–1409; *Angew. Chem.* **2001**, *113*, 1416–1455; d) P. Batail (Ed.), Special issue on Molecular Conductors, *Chem. Rev.* **2004**, *104*, 4887–5782; e) P. Frère, P. J. Skabara, *Chem. Soc. Rev.* **2005**, *34*, 69–98; f) M. Iyoda, M. Hasegawa, *Beilstein J. Org. Chem.* **2015**, *11*, 1596–1613.
- [2] A. Aviram, M. A. Ratner, *Chem. Phys. Lett.* **1974**, *29*, 277–283.
- [3] M. Bendikov, F. Wudl, D. Perepichka, *Chem. Rev.* **2004**, *104*, 4891–4945.
- [4] a) G. Ho, J. R. Heath, M. Kondratenko, D. F. Perepichka, K. Arseneault, M. Pézolet, M. R. Bryce, *Chem. Eur. J.* **2005**, *11*, 2914–2922; b) S. Leroy-Lhez, J. Baffreau, L. Perrin, E. Levillain, M. Allain, M.-J. Blesa, P. Hudhomme, *J. Org. Chem.* **2005**, *70*, 6313–6320; c) G. Zhang, D. Zhang, Y. Zhou, D. Zhu, *J. Org. Chem.* **2006**, *71*, 3970–3972; d) H. Qiu, C. Wang, J. Xu, G. Lai, Y. Shen, *Monatsh. Chem.* **2008**, *139*, 1357–1362; e) L. Jia, G. Zhang, D. Zhang, J. Xiang, W. Xu, D. Zhu, *Chem. Commun.* **2011**, *47*, 322–324; f) G. Jayamurugan, V. Gowri, D. Hernández, S. Martin, A. González-Orive, C. Dengiz, O. Dumele, F. Pérez-Murano, J.-P. Gisselbrecht, C. Boudon, W. B. Schweizer, B. Breiten, A. D. Finke, G. Jeschke, B. Bernet, L. Ruhlmann, P. Cea, F. Diederich, *Chem. Eur. J.* **2016**, *22*, 10539–10547.
- [5] a) B. Insuasty, C. Atienza, C. Seoane, N. Martín, J. Garín, J. Orduna, R. Alcalá, B. Villacampa, *J. Org. Chem.* **2004**, *69*, 6986–6995; b) J. F. Lamère, I. Malfant, A. Sournia-Saquet, P. G. Lacroix, J. M. Fabre, L. Kaboub, T. Abbaz, A.-K. Gouasmia, I. Asselberghs, K. Clays, *Chem. Mater.* **2007**, *19*, 805–815; c) M. A. Petersen, A. S. Andersson, K. Kilså, M. B. Nielsen, *Eur. J. Org. Chem.* **2009**, 1855–1858; d) J. Guasch, L. Grisanti, V. Lloveras, J. Vidal-Gancedo, M. Souto, D. C. Morales, M. Vilaseca, C. Sissa, A. Painelli, I. Ratera, C. Rovira, J. Veciana, *Angew. Chem. Int. Ed.* **2012**, *51*, 11024–11028; *Angew. Chem.* **2012**, *124*, 11186–11190; e) K. Tsujimoto, R. Ogasawara, Y. Kishi, H. Fujiwara, *New J. Chem.* **2014**, *38*, 406–418; f) Y. Geng, F. Pop, C. Yi, N. Avarvari, M. Grätzel, S. Decurtins, S.-X. Liu, *New J. Chem.* **2014**, *38*, 3629–3274; g) M. Souto, M. V. Solano, M. Jensen, D. Bendixen, F. Delchiaro, A. Giraldo, A. Painelli, J. O. Jeppesen, C. Rovira, I. Ratera, J. Veciana, *Chem. Eur. J.* **2015**, *21*, 8816–8825.
- [6] a) P. de Miguel, M. R. Bryce, L. M. Goldenberg, A. Beeby, V. Khodorkovsky, L. Shapiro, A. Niemi, A. O. Cuelloc, V. Rotell, *J. Mater. Chem.* **1998**, *8*, 71–76; b) J. L. Segura, E. M. Priego, Nazario Martín, C. Luo, D. M. Guldi, *Org. Lett.* **2000**, *2*, 4021–4024; c) P. A. Liddell, G. Kodis, L. de la Garza, J. L. Bahr, A. L. Moore, T. A. Moore, D. Gust, *Helv. Chim. Acta* **2001**, *84*, 2765–2783; d) X. Guo, D. Zhang, H. Zhang, Q. Fan, W. Xu, X. Ai, L. Fan, D. Zhu, *Tetrahedron* **2003**, *59*, 4843–4850; e) X. Guo, Z. Gan, H. Luo, Y. Araki, D. Zhang, D. Zhu, O. Ito, *J. Phys. Chem. A* **2003**, *107*, 9747–9753; f) G. Zhang, D. Zhang, X. Guo, D. Zhu, *Org. Lett.* **2004**, *6*, 1209–1212; g) S. Chopin, Z. Gan, J. Cousseau, Y. Araki, O. Ito, *J. Mater. Chem.* **2005**, *15*, 2288–2296; h) H. Lu, W. Xu, D. Zhang, C. Chen, D. Zhu, *Org. Lett.* **2005**, *7*, 4629–4632; i) X. Xiao, W. Xu, D. Zhang, H. Xu, L. Liu, D. Zhu, *New J. Chem.* **2005**, *29*, 1291–1294; j) S. Saha, E. Johansson, A. H. Flood, H.-R. Tseng, J. I. Zink, J. F. Stoddart, *Chem. Euro. J.* **2005**, *11*, 6846–6858; k) J. Baffreau, F. Dumur, P. Hudhomme, *Org. Lett.* **2006**, *8*, 1307–1310; l) F. Oswald, S. Chopin, P. de la Cruz, J. Orduna, J. Garín, A. S. D. Sandanayaka, Y. Araki, O. Ito, J. L. Delgado, J. Cousseau, F. Langa, *New J. Chem.* **2007**, *31*, 230–236; m) L. Liu, G. Zhang, W. Tan, D. Zhang, D. Zhu, *Chem. Phys. Lett.* **2008**, *465*, 230–233; n) Z. Yan, G. Zhang, D. Zhang, D. Zhu, *J. Org. Chem.* **2009**, *74*, 4375–4378; o) C. Wang, W. Tang, H. Zhong, X. Zhang, Y. Shen, *J. Hetero. Chem.* **2009**, *46*, 881–885.
- [7] a) A. S.-Schwok, M. B.-Desce, J. -M. Lehn, *J. Phys. Chem.* **1990**, *94*, 3894–3902; b) Y. Li, T. Liu, H. Liu, M.-Zhong Tian, Y. Li, *Acc. Chem. Res.* **2014**, *47*, 1186–1198.
- [8] a) J.-i. Yamada, H. Akutsu, H. Nishikawa, K. Kikuchi, *Chem. Rev.* **2004**, *104*, 5057–5083; b) Y. Misaki, *Sci. Technol. Adv. Mater.* **2009**, *10*, 024301 (22pp); c) G. Saito, Y. Yoshida, *Chem. Rec.* **2011**, *11*, 124–145.
- [9] a) S. Kato, F. Diederich, *Chem. Commun.* **2010**, *46*, 1994–2006; b) P.-A. Bouit, C. Villegas, J. L. Delgado, P. M. Viruela, R. Pou-Amerigo, E. Orti, N. Martín, *Org. Lett.* **2011**, *13*, 604–607; c) T. Shoji, S. Ito, T. Okujima, N. Morita, *Org. Biomol. Chem.* **2012**, *10*, 8308–8313; d) K. Guo, K. Yan, X. Lu, Y. Qiu, Z. Liu, J. Sun, F. Yan, W. Guo, S. Yang, *Org. Lett.* **2012**, *14*, 2214–2217; e) H. Hopf, M. S. Sherburn, *Angew. Chem. Int. Ed.* **2012**, *51*, 2298 – 2338; *Angew. Chem.* **2012**, *124*, 2346–2389.
- [10] T. J. Chow, N. R. Chiu, H. C. Chen, C. Y. Chen, W. S. Yu, Y. M. Cheng, C. C. Cheng, C. P. Chang, P. T. Chou, *Tetrahedron* **2003**, *59*, 5719–5730.
- [11] a) *Cyclophanes vol. 1*, vol. 2, (Ed.: P. M. Keehn, S. M. Rosenfeld), Academic Press, New York, **1983**; b) *Cyclophanes I, Topics in Current Chemistry 113*, (Ed.: L. Rossa, F. Vögtle, V. Boekelheide, I. Tabushi, K. Yamamura), Springer-Verlag, Berlin, **1983**; c) *Cyclophanes II, Topics in Current Chemistry 115*, (Ed.: F. Vögtle), Springer-Verlag, Berlin, **1983**; d) F. Diederich *Cyclophanes, Monographs in Supramolecular Chemistry*, The Royal Society of Chemistry, London, **1991**; e) *Cyclophane Chemistry*, (Ed.: F. Vögtle), Wiley, New York, **1993**.
- [12] a) H. A. Staab, U. Zapf, A. Gurke, *Angew. Chem. Int. Ed. Engl.* **1977**, *16*, 801–803; *Angew. Chem.* **1977**, *89*, 841–842; b) H. A. Staab, U. Zapf, *Angew. Chem. Int. Ed. Engl.* **1978**, *17*, 757–758; *Angew. Chem.* **1978**, *90*, 807–808; c) H. A. Staab, G. H. Knaus, H. E. Henke, C. Krieger, *Chem. Ber.* **1983**, *116*, 2785–2807; d) H. A. Staab, R. Hinz, G. H. Knaus, C. Krieger, *Chem. Ber.* **1983**, *116*, 2835–2847; e) H. A. Staab, C. Krieger, P. Wahl, K. Y. Kay, *Chem. Ber.* **1987**, *120*, 551–558; f) H. A. Staab, P. Wahl, K. Y. Kay, *Chem. Ber.* **1987**, *120*, 541–549; g) H. A. Staab, M. Tercel, R. Fischer, C. Krieger, *Angew. Chem. Int. Ed. Engl.* **1994**, *33*, 1463–1464; *Angew. Chem.* **1994**, *106*, 1531–1534; h) H. A. Staab, A. Feurer, R. Hauck, *Angew. Chem. Int. Ed. Engl.* **1994**, *33*, 2428–2431; *Angew. Chem.* **1994**, *106*, 2542–2545.
- [13] a) H. Tatemitsu, B. Natsume, M. Yoshida, Y. Sakata, S. Misumi, *Tetrahedron Lett.* **1978**, *19*, 3459–3462; b) H. Machida, H. Tatemitsu, T. Otsubo, Y. Sakata, S. Misumi, *Bull. Chem. Soc. Jpn.* **1980**, *53*, 2943–2952.
- [14] a) T. Shinmyozu, T. Inazu, T. Yoshino, *Chem. Lett.* **1977**, 1347 1350; b) M. Watanabe, K. Goto, M. Shibahara, T. Shinmyozu, *J. Org. Chem.* **2010**, *75*, 6104–6114; c) M. Watanabe, K. Goto, M. Fujitsuka, S. Tojo, T. Majima, T. Shinmyozu, *Bull. Chem. Soc. Jpn.* **2010**, *83*, 1155–1161.
- [15] a) Y. J. Chang, M. Watanabe, Po-T. Chou, T. J. Chow, *Chem. Commun.* **2012**, *48*, 726–728; b) C. H. Huang, Y. J. Chang, *Tetrahedron Lett.* **2014**, *55*, 4938–4942; c) Y. Yang, G. Zhang, C. Yu, J. Yao, Z. Liu, D. Zhang, *New J. Chem.* **2015**, *39*, 6421–6427; d) S. Park, J. H. Heo, C. H. Cheon, H. Kim, S. H. Im, H. J. Son, *J. Mater. Chem. A* **2015**, *3*, 24215–24220.
- [16] a) J. Zyss, I. Ledoux, S. Volkov, V. Chernyak, S. Mukamel, G. P. Bartholomew, G. C. Bazan, *J. Am. Chem. Soc.* **2000**, *122*, 11956–11962; b) G. P. Bartholomew, I. Ledoux, S. Mukamel, G. C. Bazan, J. Zyss, *J. Am. Chem. Soc.* **2002**, *124*, 13480–13485; c) G. C.

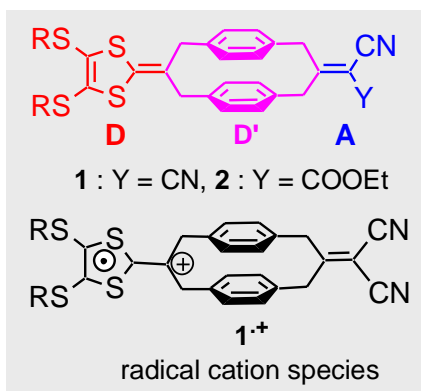
- 1 Bazan, *J. Org. Chem.* **2007**, *72*, 8615–8635; d) F. Kajzar, L. N. Puntus,
2 I. Rau, E. V. Sergeeva, K. A. Lyssenko, *Mol. Cryst. Liq. Cryst.* **2012**,
3 *554*, 22–30; e) E. V. Sergeeva, L. N. Puntus, F. Kajzar, I. Rau, B.
4 Sahraoui, I. S. Pekareva, K. Y. Suponitsky, I. S. Bushmarinov, K. A.
5 Lyssenko, *Opt. Mater.* **2013**, *36*, 47–52; f) M. Fujitsuka, T. Miyazaki, C.
6 Lu, T. Shinmyozu, T. Majima, *J. Phys. Chem. A* **2016**, *120*, 1184–1189.
7 [17] a) B. König, J. Heinze, K. Meerholz, A. de Meijere, *Angew. Chem. Int.*
8 *Ed. Engl.* **1991**, *30*, 1361–1363; *Angew. Chem.* **1991**, *103*, 1350–1351;
9 b) F. Gerson, M. Scholz, A. de Meijere, B. König, J. Heinze, K.
10 Meerholz, *Helv. Chem. Acta* **1992**, *75*, 2307–2316; c) B. König, A. de
11 Meijere, *Chem. Ber.* **1992**, *125*, 1895–1897; d) O. Reiser, B. König, K.
12 Meerholz, J. Heinze, T. Wellauer, F. Gerson, R. Frim, M. Rabinovitz, A.
13 de Meijere, *J. Am. Chem. Soc.* **1993**, *115*, 3511–3518; e) K. Sako, Y.
14 Mase, Y. Kato, T. Iwanaga, T. Shinmyozu, H. Takemura, M. Ito, K.
15 Sasaki, H. Tatemitsu, *Tetrahedron. Lett.* **2006**, *47*, 9151–9154.
16 [18] A. J. Moore, M. R. Bryce, *Synthesis* **1991**, 26–28.
17 [19] a) K. Kurosawa, M. Suenaga, T. Inazu, T. Yoshino, *Tetrahedron Lett.*
18 **1982**, *23*, 5335–5338; b) W. Matsuda-Sentou, T. Shinmyozu, *Eur. J.*
19 *Org. Chem.* **2000**, 3195–3203.
20 [20] A. J. Moore, M. R. Bryce, P. J. Skabara, A. S. Batsanov, L. M.
21 Goldenberg, J. A. K. Howard, *J. Chem. Soc., Perkin Trans. 1* **1997**,
22 3443–3450.
23 [21] T. Miyazaki, M. Shibahara, J. Fujishige, M. Watanabe, K. Goto, T.
24 Shinmyozu, *J. Org. Chem.* **2014**, *79*, 11440–11453.
25 [22] The molecular orbital calculations were carried out using the Gaussian
26 09 Revision C.01, M. J. Frisch et al., Gaussian, Inc., Wallingford CT,
27 2010.
28 [23] C. M. Cardona, W. Li, A. E. Kaifer, D. Stockdale, G. C. Banzan, *Adv.*
29 *Mater.* **2011**, *23*, 2367–2371.
30 [24] Notes: MS The mass spectrum of electrolytic oxidized product at +0.8V
31 (vs. Ag/AgNO₃) for 5min. were observed two major ion peaks of the
32 neutral DTF reference **6** (m/z 388) and the DTF dimer derivatives (m/z
33 630). From the major ion peak, the molecular formula of the DTF dimer
34 derivative is estimated C₂₆H₃₀O₂S₈. The DTF dimer derivative is
35 suggested to be formed by dimerization of DTF radical cations to
36 generate DTF dication with elimination of two benzyl groups, and
37 addition of water (Scheme 1S). Some references of DTF radical cation
38 dimerization are as follows; a) P. Hapiot, D. Lorcy, A. Tallec, R. Carlier,
39 A. Robert, *J. Phys. Chem.* **1996**, *100*, 14823–14827; b) S. González, N.
40 Martín, L. Sánchez, J. L. Segura, C. Seoane, I. Fonseca, F. H. Cano, J.
41 Sedó, J. Vidal-Gancedo, C. Rovira, *J. Org. Chem.* **1999**, *64*,
42 3498–3506; c) M. Guerro, R. Carlier, K. Boubekeur, D. Lorcy, P. Hapiot,
43 *J. Am. Chem. Soc.* **2003**, *125*, 3159–3167; d) Pierre Frère, P. J.
44 Skabara, *Chem. Soc. Rev.* **2005**, *34*, 69–98.
45 [25] C. Kabuto, S. Akine, T. Nemoto, E. Kwon, *J. Cryst. Soc. Jpn.* **2009**, *51*,
46 218–224.
47
48
49
50
51
52
53
54
55
56
57
58
59
60
61
62
63
64
65

Entry for the Table of Contents (Please choose one layout)

Layout 1:

FULL PAPER

The new DTF(D)-[3.3]PCP(D')-DCM or ECM (**1**, **2**) triads, based on [3.3]paracyclophane ([3.3]PCP) as a bridge with electron-donating property (D') with 1,4-dithiafulvene (DTF) as a donor and dicyanomethylene (DCM) or an ethoxycarbonyl-cyanomethylene (ECM) as an acceptor were synthesized. The D-B(D')-A triad **1** can stabilize the DTF radical cation by introduction of rigid [3.3]PCP without substitution of sterically bulky substituents.



K. Sako,* T. Hasegawa, H. Onda, M. Shiotsuka, M. Watanabe, T. Shinmyozu, S. Tojo, M. Fujitsuka, T. Majima, Y. Hirao, T. Kubo, T. Iwanaga, S. Toyota, and H. Takemura

Page No. – Page No.

Donor-Donor'-Acceptor Triads based on [3.3]Paracyclophane with 1,4-Dithiafulvene Donor and Cyanomethylene Acceptor: Synthesis, Structure, Electro- and Photo-physical Properties

1
2
3
4
5
6
7
8
9
10
11
12
13
14
15
16
17
18
19
20
21
22
23
24
25
26
27
28
29
30
31
32
33
34
35
36
37
38
39
40
41
42
43
44
45
46
47
48
49
50
51
52
53
54
55
56
57
58
59
60
61
62
63
64
65